

# A new spinfoam vertex for quantum gravity

Etera R. Livine<sup>a</sup> and Simone Speziale<sup>b\*</sup>

<sup>a</sup>*Laboratoire de Physique, ENS Lyon, 46 Allée d'Italie, 69364 Lyon, France*

<sup>b</sup>*Perimeter Institute, 31 Caroline St. N, Waterloo, ON N2L 2Y5, Canada*

February 8, 2022

## Abstract

We introduce a new spinfoam vertex to be used in models of 4d quantum gravity based on  $SU(2)$  and  $SO(4)$  BF theory plus constraints. It can be seen as the conventional vertex of  $SU(2)$  BF theory, the  $15j$  symbol, in a particular basis constructed using  $SU(2)$  coherent states. This basis makes the geometric interpretation of the variables transparent: they are the vectors normal to the triangles within each tetrahedron. We study the condition under which these states can be considered semiclassical, and we show that the semiclassical ones dominate the evaluation of quantum correlations. Finally, we describe how the constraints reducing BF to gravity can be directly written in terms of the new variables, and how the semiclassicality of the states might improve understanding the correct way to implement the constraints.

## 1 Introduction

The spinfoam formalism for loop quantum gravity (LQG) [1] is a covariant approach to the definition of the dynamics of quantum General Relativity (GR). It provides transition amplitudes between spin network states. The most studied example in the literature is the Barrett–Crane (BC) model [2]. This model has interesting aspects, such as the inclusion of Regge calculus in a precise way, but it can not be considered a complete proposal. In particular, recent developments on the semiclassical limit show that it does not give the full correct dynamics for the free graviton propagator [3]. In this paper we introduce a new model that can be taken as the starting point for the definition of a better behaved dynamics.

Most spinfoam models, including BC, are based on BF theory, a topological theory whose relevance for 4d quantum gravity has long been conjectured [4], and has been exploited in a number of ways. In constructing a specific model for quantum gravity, there is a key difficulty of quantum BF theory that has to be overcome: not all the variables

---

\*etera.livine@ens-lyon.fr, sspeziale@perimeterinstitute.ca

describing a classical geometry turn out to commute. This fact has two important consequences. The first is that there is in general no classical geometry associated to the spin network in the boundary of the spinfoam. This leads immediately to the problem of finding semiclassical quantum states that approximate a given classical geometry, in the sense in which wave packets or coherent states approximate classical configurations in ordinary quantum theory. This is the problem of defining “coherent states” for LQG, which has raised an increasing interest over the last few years [5, 6]. The second consequence concerns the definition of the dynamics. This is typically obtained by constraining the BF theory, a mechanism well understood classically, but still unsettled at the quantum level. The constraints involve non-commuting variables, and the way to properly impose them is still an open issue. In particular, it can be argued that the specific procedure leading to the BC model imposes them too strongly, a fact which also complicates a proper match with the states of the canonical theory (LQG) living on the boundary. For a recent discussion of this, see [7]. Notice that these key difficulties are present for both lorentzian and euclidean signatures.

Here we consider a definition of the partition function of  $SU(2)$  BF theory on a Regge triangulation (for a review see for instance [1]), where the dynamical variables entering the sum have a clear semiclassical interpretation: they are the normal vectors  $\vec{n}_{t,\tau}$  associated to triangles  $t$  within a tetrahedron  $\tau$ . The classical geometry of this discrete manifold (areas, angles, volumes, etc.) can be described in a transparent way in these variables, provided they satisfy a constraint for each tetrahedron of the triangulation. This constraint is the closure condition, that says that the sum of the four normals associated to each tetrahedron must vanish. If this condition is satisfied, this new choice of variables positively addresses the issues described above, in the following way. First of all, from the boundary point of view, each tetrahedron corresponds to a node of the boundary spin network. As we show below, the states associated to the new variables are linear superpositions of the conventional ones, with the property of minimizing the uncertainty of the non commuting operators: they thus provide a solution to the problem of finding coherent states. Upon satisfying the closure condition, the states are coherent and carry a given classical geometry. Secondly, as far as the dynamics is concerned, the constraints reducing BF theory to GR are functions of the full bivectorial structure of the  $B$  field. In our model this structure is related to the vectors  $\vec{n}_{t,\tau}$  in a precise way. We describe how this improves the construction of the constraints at the quantum level. We postpone a more detailed analysis of the constraints for further work.

A key point of this approach is the closure condition. As mentioned above, this is crucial for the semiclassical interpretation of the states. This is not satisfied by all the states entering the partition function. Yet one of the main results of this paper is to show that quantum correlations are dominated by the semiclassical states in the large spin limit. The key to this mechanism lies in the fact that the coherent states we introduce are not normalized, and the configurations maximizing the norm are the ones satisfying the closure condition. To prove this, we write the norm as an integral over  $SU(2)$ , which we are able to solve explicitly in particular cases. In the general case, we evaluate the integral using the saddle point approximation, and show that the configurations satisfying

the closure condition are exponentially dominating. All our calculations are supported by numerical simulations, some of which are reported in the Appendix. Remarkably, the approximation is accurate even for small spins, and agrees to three digits with the numerics at spins of order 100.

The results we obtain are valid for  $SU(2)$  BF theory, but can be straightforwardly extended to  $Spin(4)$ , and the same logic applied to any Lie group, including noncompact cases which are of interest for lorentzian signatures. We postpone such developments for further work, once the approach considered here proves useful to solve the problems described above.

This paper is organized as follows. In Section 2, we introduce the new vertex amplitude, and describe how it can be obtained following the conventional spinfoam quantization of BF theory. The new variables are normal vectors associated to the triangles, and the new vertex built out of coherent intertwiners. In Section 3 we study the norm of the coherent intertwiners, and show that it is exponentially bigger when the closure condition holds, thus making semiclassical states dominate the partition function. In Section 4 we describe the coherent tetrahedron in the conventional basis. In Section 5 we discuss how the new vertex can be used as a starting point for models of quantum gravity. We summarize our results in Section 6.

Throughout the paper we use unit  $\hbar = G = 1$ .

## 2 The new vertex amplitude

In this Section we describe the vertex amplitude that characterizes our spinfoam model. The vertex can be constructed using the conventional procedure for the spinfoam quantization of  $SU(2)$  BF theory. We refer to the literature for details (see for instance [1]), and focus here only on the aspect which is relevant to construct the new vertex.

Recall that there is a vector space  $\mathcal{H}_0 := \text{Inv} \left[ \bigotimes_{i=1}^F \mathcal{H}_{j_i} \right]$ , on which  $(\sum_i \vec{J}_i)^2 \equiv 0$ , associated with each edge of the spinfoam. Here the half-integer (spin)  $j$  labels the irreducible representations (irreps) of  $SU(2)$ , and  $F$  is the number of faces around the edge. If the spinfoam is defined on a Regge triangulation,  $F \equiv 4$  for every edge, yet the considerations of this paper apply to any value of  $F$ . The spinfoam quantization assigns to each edge an integral over the group, that is evaluated by inserting in  $\mathcal{H}_0$  the resolution of identity

$$\mathbb{1}_{\mathcal{H}_0} = \sum_{i_1 \dots i_{F-3}} |j_1 \dots j_F, i_1 \dots i_{F-3}\rangle \langle j_1 \dots j_F, i_1 \dots i_{F-3}|. \quad (1)$$

The labels  $i$  are called intertwiners, and the sums run over all half-integer values allowed by the Clebsch-Gordan conditions. Taking into account the combinatorial structure of the Regge triangulation (four triangles  $t$  in every tetrahedron  $\tau$ , five tetrahedra in every 4-simplex  $\sigma$ ), one ends up with the partition function,

$$Z = \sum_{\{j_t\}} \sum_{\{i_\tau\}} \prod_t d_{j_t} \prod_\sigma A_\sigma(j_t, i_\tau), \quad (2)$$

where  $d_j = 2j + 1$  is the dimension of the irrep  $j$ , and the vertex amplitude is  $A_\sigma(j_t, i_\tau) = \{15j\}$ , a well known object from the recoupling theory of  $SU(2)$ .

This partition function endows each 4-simplex with 15 quantum numbers, the ten irrep labels  $j_t$  and the five intertwiner labels  $i_\tau$ . Using LQG operators associated with the boundary of the 4-simplex, the ten  $j_t$  can be interpreted as areas of the ten triangles in the 4-simplex while the five  $i_\tau$  give 3d dihedral angles between triangles (one – out of the possible six – for each tetrahedron). On the other hand, the complete characterization of a classical geometry on the 3d boundary requires 20 parameters, such as the ten areas plus two dihedral angles for each tetrahedron (see next Section for more details). Therefore the quantum numbers of the partition function are not enough to characterize a classical geometry.

To overcome these difficulties, we propose to write the same partition function in different variables, which will endow each 4-simplex with enough geometric information.

The key observation is that  $SU(2)$  coherent states  $|j, \hat{n}\rangle$  (here  $\hat{n}$  is a unit vector on the two-sphere  $\mathcal{S}^2$  – see below and Appendix A for details) provide a (overcomplete) basis for the irreps. Given an irrep  $j$ , the resolution of the identity in this representation can indeed be written as  $\mathbb{1}_j = d_j \int d^2\hat{n} |j, \hat{n}\rangle \langle j, \hat{n}|$ , where  $d^2\hat{n}$  is the normalized measure on  $\mathcal{S}^2$ . By group averaging the tensor product of  $F$  coherent states, we obtain a vector

$$|\underline{j}, \underline{\hat{n}}\rangle_0 := \int_{SU(2)} dh \otimes_{i=1}^F h |j_i, \hat{n}_i\rangle$$

in  $\mathcal{H}_0$ . Here we denoted  $\underline{j}$  and  $\underline{\hat{n}}$  the collections of all  $j_i$ 's and  $\hat{n}_i$ 's. The set of all these vectors when varying the  $\hat{n}_i$ 's forms an overcomplete basis in  $\mathcal{H}_0$ . Using this basis the resolution of the identity in  $\mathcal{H}_0$  can be written as

$$\begin{aligned} \mathbb{1}_{\mathcal{H}_0} &= \int \prod_{i=1}^F d^2\hat{n}_i d_{j_i} |\underline{j}, \underline{\hat{n}}\rangle_0 \langle \underline{j}, \underline{\hat{n}}|_0 = \\ &= \int \prod_{i=1}^F d^2\hat{n}_i d_{j_i} \int dh \int dh' h |j_i, \hat{n}_i\rangle \langle j_i, \hat{n}_i| h'. \end{aligned} \quad (3)$$

This formula can be used in the edge integrations instead of (1). The combinatorics is the same as before. In particular, notice that (3) assigns to a triangle  $t$  a normal  $\hat{n}_t(\tau)$  for each tetrahedron sharing  $t$ . Within a single 4-simplex, there are two tetrahedra sharing a triangle, which we denote  $u(t)$  and  $d(t)$ . Furthermore, (3) assigns two group integrals to each tetrahedron, one for each 4-simplex sharing it. Taking also into account the  $d_j$  factors in (3) and using the conventional spinfoam procedure, one gets

$$Z = \sum_{\{j_t\}} \int \prod_{t,\tau} d^2\hat{n}_{t,\tau} \prod_t d_{j_t}^3 \prod_\sigma A_\sigma(j_t, \hat{n}_{t,\epsilon(t)}) \quad (4)$$

where the new vertex is

$$A_\sigma = \int \prod_\tau dh_\tau \prod_t \langle j_t, \hat{n}_{t,u(t)} | h_{u(t)}^{-1} h_{d(t)} | j_t, \hat{n}_{t,d(t)} \rangle. \quad (5)$$

Let us add a few comments.

- The new vertex gives a quantization of BF theory in terms of the variables  $j_t$  and  $\hat{n}_{t,\tau(t)}$ . Together, these represent the full bivector  $B_{\mu\nu}^i(x)$  discretized on triangles belonging to tetrahedra. Taking the  $B$  field constant on each tetrahedron, the discretization and quantization procedures can be schematically summarized as follows,

$$B_{\mu\nu}^i(x) \xrightarrow{\text{discr}} B_t^i(\tau) := \int_t B_{\mu\nu}^i(x) dx^\mu \wedge dx^\nu \xrightarrow{\text{quant}} j_t \hat{n}_{t,\tau}. \quad (6)$$

In the quantum theory, the field  $B_{\mu\nu}^i(x)$  is represented by a vector  $j_t \hat{n}_{t,\tau(t)}$  associated to each triangle in a given tetrahedron. The set of all these vectors can be used to describe a classical discrete geometry.

On the other hand, the conventional quantization of BF theory differs in the quantization step, which reads

$$B_t^i \xrightarrow{\text{quant}} J_t^i, \quad (7)$$

where  $\vec{J}_t$  are SU(2) generators associated to each triangle. Consequently the variables entering the partition function (2) are irrep labels  $j_t$  and intertwiner labels  $i_\tau$ . The first variables are related to discretization of the modulus of  $B$ , and thus to the area of triangles. The intertwiner labels are related to *one* angle (out of six) for each tetrahedron. Therefore in these variables a classical geometry is hidden, and this in turn makes it hard to implement the dynamics, as we discuss below in Section 5.

- This vertex can be used directly for SU(2) BF theory, and straightforwardly generalized to the Spin(4) case, exploiting the homomorphism  $\text{Spin}(4) = \text{SU}(2) \times \text{SU}(2)$ . In particular, (6) becomes

$$B_{\mu\nu}^{IJ}(x) \xrightarrow{\text{discr}} B_t^{IJ}(\tau) := \int_t B_{\mu\nu}^{IJ}(x) dx^\mu \wedge dx^\nu \xrightarrow{\text{quant}} j_t^+ \hat{n}_{t,\tau}^+ \oplus j_t^- \hat{n}_{t,\tau}^-. \quad (8)$$

- There is a simple relation between this vertex and the one given in (2) which is the one usually used. Since all we did is simply a change of basis, (5) can be written as a linear combination of  $\{15j\}$ 's as we will see in more details in Section 4.
- The BC vertex can be obtained from (5): performing the  $d^2 \hat{n}_i$  integrations with the condition  $\hat{n}_{t,u(t)} \equiv \hat{n}_{t,d(t)}$  (namely inserting terms  $\delta(\hat{n}_{t,u(t)} - \hat{n}_{t,d(t)})$  in (4)), we indeed obtain the BC vertex in its integral representation [8],

$$A_{\text{BC}} = \int_{\text{SU}(2)} \prod_\tau dh_\tau \prod_t \frac{1}{d_{j_t}} \chi^{(j_t)}(h_{u(t)}^{-1} h_{d(t)}). \quad (9)$$

To understand the geometry of this new vertex amplitude, it is crucial to study its asymptotic behaviour in the large spin limit.<sup>1</sup> In the rest of this paper, we begin the analysis of this limit, by studying in details the behavior of the states  $|j, \hat{n}\rangle_0$  entering (5). The full asymptotics of the vertex will be reported elsewhere. Nonetheless, it will become clear from the rest of the paper that the large spin limit of this integral is dominated by values of the group elements such that the factors of the integrand in (5) are close to one, namely such that

$$|j_t, \hat{n}_{t,u(t)}\rangle = h_{u(t)}^{-1} h_{d(t)} |j_t, \hat{n}_{t,d(t)}\rangle. \quad (10)$$

This has a compelling geometric interpretation. Recall that  $\hat{n}_{t,u(t)}$  and  $\hat{n}_{t,d(t)}$  are the normals to the same triangle as seen from the two tetrahedra sharing it. Then (10) means that they are changed into one another by a gravitational holonomy.

This is in contrast with the BC model, which fixes  $\hat{n}_{t,u(t)} \equiv \hat{n}_{t,d(t)}$ , thus not allowing any gravitational parallel transport between tetrahedra. This is another way of seeing the well known problem that the BC model has not enough degrees of freedom. We will come back to this point in Section 5, where we discuss how this vertex can be taken as the starting point for quantum gravity models.

### 3 Coherent intertwiners

In this Section we focus on the building blocks of the new vertex, namely the states  $|j, \hat{n}\rangle_0$  associated to the tetrahedra entering (3). Before studying the details of the mathematical structure of these states, let us discuss their physical meaning. In the canonical picture, a tetrahedron is dual to a 4-valent node in a spin network. More in general, when the edge of the spinfoam is on the boundary, there is a one-to-one correspondence between the number of faces  $F$  around it, and the valence  $V$  of the node of the boundary spin network. Given a discrete atom of space dual to the node with  $V$  faces, its classical geometry can be entirely determined using the  $V$  areas and  $2(V - 3)$  angles between them. Alternatively, one can use the (non-unit) normal vectors  $\vec{n}_i$  associated with the faces, constrained to *close*, namely to satisfy  $\sum_i \vec{n}_i = 0$ .

On the other hand, the conventional basis used in (1) gives quantum numbers for  $V$  areas but only  $V - 3$  angles. This is immediate from the fact that one associates  $SU(2)$  generators  $\vec{J}_i$  with each face [9], and only  $V - 3$  of the possible scalar products  $\vec{J}_i \cdot \vec{J}_k$  commute among each other. Thus half the classical angles are missing. To solve this problem, we argue that the states  $|j, \hat{n}\rangle_0$  carry enough information to describe a classical geometry for the discrete atom of space dual to the node. In particular, we interpret the vectors  $j_i \hat{n}_i$  precisely with the meaning of normal vectors  $\vec{n}_i$  to the triangle, and we read the geometry off them as described above. This requires the vectors to satisfy the

---

<sup>1</sup>The reasons why the large spin limit is relevant to discuss the dynamics of spinfoams is largely discussed in the literature (see for instance [1]). The main reason is that this limit appears to be related to Regge calculus, a discrete version to classical GR.

following constraint:

$$\vec{N} = \sum_{i=1}^V j_i \hat{n}_i = 0. \quad (11)$$

This *closure condition* will be studied in detail in the rest of this Section. If (11) holds, all classical geometric observables can be parametrized as  $\mathcal{O}(\{j_i \hat{n}_i\})$ .

This is the physical picture we consider. To describe the mathematical details, let us recall basic properties of the  $SU(2)$  coherent states (for details see the Appendix A). A coherent state is obtained via the group action on the highest weight state,

$$|j, \hat{n}\rangle = g(\hat{n})|j, j\rangle, \quad (12)$$

where  $g(\hat{n})$  is a group element rotating the north pole  $\hat{z} \equiv (0, 0, 1)$  to the unit vector  $\hat{n}$  (and such that its rotation axis is orthogonal to  $\hat{z}$ ). These coherent states are semiclassical in the sense that they localize the direction  $\hat{n}$  of the angular momentum. We have  $\langle j, \hat{n} | \vec{J} | j, \hat{n} \rangle = j \hat{n}$  and relative uncertainty  $\Delta \sim 1/\sqrt{j}$  vanishing in the large spin limit (see Appendix B). As  $|j, j\rangle$  has direction  $z$  with minimal uncertainty,  $|j, \hat{n}\rangle$  has direction  $\hat{n}$  with minimal uncertainty.

This localization property is preserved by the tensor product of irreps  $\otimes_i |j_i, \hat{n}_i\rangle$ : in the large spin limit we have for instance  $\langle \vec{J}_i \cdot \vec{J}_k \rangle \simeq j_i j_k \hat{n}_i \cdot \hat{n}_k$  for any  $i$  and  $k$ . More in general any operator  $\hat{\mathcal{O}}(\{\vec{J}_i\})$  on the tensor product of coherent states satisfies

$$\langle \hat{\mathcal{O}}(\{\vec{J}_i\}) \rangle \simeq \mathcal{O}(\{j_i \hat{n}_i\}) \quad (13)$$

with vanishing relative uncertainty.

So far, the  $\hat{n}_i$ 's are completely free parameters. If the closure condition (11) holds, (13) tells us that the states admit a semiclassical interpretation. Consequently, states in  $\bigotimes_{i=1}^V \mathcal{H}_{j_i}$  satisfying (11) can be considered semiclassical. Yet they cannot be used in the partition function: the tensor product of coherent states must be projected on the invariant subspace  $\mathcal{H}_0$ , in order to implement gauge invariance. This can be achieved by group averaging, as anticipated in the previous Section, and the resulting states written as a linear combination of the conventional basis of intertwiners are

$$\mathcal{H}_0 \ni |\underline{j}, \underline{\hat{n}}\rangle_0 := \int dh \otimes_{i=1}^V h |j_i, \hat{n}_i\rangle = \sum_{i_1 \dots i_{V-3}} c_{i_1 \dots i_{V-3}}(j_i, \hat{n}_i) |j_1 \dots j_V, i_1 \dots i_{V-3}\rangle. \quad (14)$$

We call these states coherent intertwiners. The explicit form of the  $c_{i_1 \dots i_{V-3}}$  coefficients is reported in the Appendix A, but it will not be relevant for the rest of the paper. In Section 4 below we will study their asymptotics in the 4-valent case.

Crucially, (13) holds on the states  $|\underline{j}, \underline{\hat{n}}\rangle_0$  (see Appendix B), thus group averaging does not spoil the semiclassical interpretation of these states in the large spin limit. But what is more important, group averaging correlates the  $\hat{n}_i$ 's, making the state sensitive to (11). Indeed, notice that a state in  $\mathcal{H}_0$  satisfies  $(\sum_i \vec{J}_i)^2 = 0$  but not necessarily the closure condition. The main result of this paper is to show that the states satisfying (11) have

an exponentially bigger norm in the large spin limit. Therefore every state (14) enters the partition function (4), but quantum correlations will be dominated by semiclassical states in the large spin limit. We can then say that projecting onto  $\mathcal{H}_0$  does not force the  $V$ -simplex to close identically, but it does imply that closed simplices dominate the dynamics.

### 3.1 The closure condition

The key for the mechanism is the following: the coherent interwiner states (14) are not normalized, and the norm is a function of the  $\hat{n}_i$ ,

$$f(\hat{n}_i) := {}_0\langle \underline{j}, \underline{\hat{n}} | \underline{j}, \underline{\hat{n}} \rangle_0 = \int dh \langle j_i, \hat{n}_i | h^{\otimes V} | j_i, \hat{n}_i \rangle \neq 1. \quad (15)$$

Consequently, the relative weight of these states will depend on the configuration of the  $\hat{n}_i$ . As we show below, the norm is exponentially smaller when the closure condition (11) is not satisfied.

To give a simple picture of the way this happens, let us first consider the trivial case of a bivalent node. In this case, the norm (15) can be straightforwardly evaluated using the explicit values of the Clebsch-Gordan coefficients. Using  $|j_i, \hat{n}_i\rangle = g_i |j_i, j_i\rangle$ , we can write

$$\langle j_i, \hat{n}_i | h | j_i, \hat{n}_i \rangle = D_{jk}^{(j_i)}(g_i^{-1}) D_{kl}^{(j_i)}(h) D_{lj_i}^{(j_i)}(g_i). \quad (16)$$

The integration over  $h$  in (15) gives the orthogonality condition for the Clebsch-Gordan coefficients,

$$\int dh D_{kl}^{(j_1)}(h) D_{mn}^{(j_2)}(h) = \frac{\delta^{j_1 j_2}}{d_{j_1}} \delta_{k,-m} \delta_{l,-n}, \quad (17)$$

and we get  $f(\hat{n}_1, \hat{n}_2) = \frac{\delta^{j_1 j_2}}{d_{j_1}} \left| D_{j_1, -j_1}^{(j_1)}(g_1^{-1} g_2) \right|^2$ . This matrix element can be evaluated starting from the fundamental representation. As we show in the Appendix B, we have

$$\left| D_{j_1, -j_1}^{(j_1)}(g_1^{-1} g_2) \right|^2 = \left| \langle + | g_1^{-1} g_2 | - \rangle \right|^{4j_1} = \left( 1 - \frac{1}{4} (\hat{n}_1 + \hat{n}_2)^2 \right)^{2j_1}. \quad (18)$$

Defining  $J = \sum_i j_i$ , we conclude that

$$f(\hat{n}_1, \hat{n}_2) = \frac{\delta^{j_1 j_2}}{d_{j_1}} \left( 1 - \frac{\vec{N}^2}{J^2} \right)^{2j_1}. \quad (19)$$

As  $\vec{N}^2 \leq J^2$ , we see that in the large spin limit the norm vanishes exponentially, unless the closure condition is satisfied, in which case it vanishes with an inverse power law. Consequently, the norm of the states satisfying the closure condition becomes exponentially bigger than the others.

Notice that in the bivalent case, the closure condition means that the two vectors are antiparallel. The situation is analogous for the trivalent case: closed configurations

will correspond to three coplanar vectors. It is only for valence four or higher that the geometry of the problem becomes more interesting, and one has closed configurations spanning 3d space. However, the configurations where the vectors are all aligned are still present. Since such configurations fail to produce 3d structures, we refer to them as degenerate.

For nodes with higher valence we expect a result analogous to (19). However the analysis is far more intricate, the reason being that now when we use (16) we obtain an integral  $\int dh \prod_i D_{m_i n_i}^{(j_i)}(h)$  of  $V$  representation matrices, and in general we have no simple formula for the (generalized) Clebsch-Gordan coefficients (see Appendix A) appearing from this integration. It is then simpler to study the norm explicitly using the fact that (see Appendix B)

$$\langle j, j | g(\hat{n})^{-1} h g(\hat{n}) | j, j \rangle = \left( \langle \frac{1}{2}, + | g(\hat{n})^{-1} h g(\hat{n}) | \frac{1}{2}, + \rangle \right)^{2j} = (\cos \gamma + i \sin \gamma \hat{u} \cdot \hat{n})^{2j}, \quad (20)$$

where we parametrized  $SU(2)$  group elements as

$$h(\gamma, \hat{u}) = \cos \gamma \mathbb{1} + i \sin \gamma \hat{u} \cdot \vec{\sigma}, \quad \gamma \in [0, \pi], \quad \hat{u} \in \mathcal{S}^2. \quad (21)$$

It is convenient to introduce the vector  $\vec{p} = \sin \gamma \hat{u}$ . In these variables, the Haar measure splits into two integrals over the unit three-ball  $B : |\vec{p}| \leq 1$ , corresponding to the northern (say  $B_+$ ) and southern (say  $B_-$ ) “hemispheres” of  $SU(2) \simeq S^3$ ,

$$\int_{SU(2)} dh = \frac{1}{2\pi^2} \sum_{\eta=\pm} \int_{B_\eta} \frac{d^3 \vec{p}}{\sqrt{1 - \vec{p}^2}}.$$

We then write (15) as

$$f(\hat{n}_i) = \frac{1}{2\pi^2} \sum_{\eta=\pm} \int_{B_\eta} \frac{d^3 \vec{p}}{\sqrt{1 - \vec{p}^2}} \prod_{i=1}^V (p_\eta + i \vec{p} \cdot \hat{n}_i)^{2j_i}. \quad (22)$$

where  $p_\eta = \eta \sqrt{1 - \vec{p}^2}$  in  $B_\eta$ . It is a triple integral depending on  $3V$  parameters. Notice that the measure tends to locate the integral on the boundary  $|\vec{p}| = 1$  of the integration domain, whereas the integrand tends to locate it on the origin  $|\vec{p}| = 0$ . In the large spin limit, the latter behaviour will of course dominate. Since we are interested in the asymptotic behavior of this norm, it is enough to study its saddle point approximation in the large spin limit. In the Appendix C we discuss the exact evaluation of the norm.

### 3.2 Saddle point analysis

We want to study the behavior of (22) in the large spin limit. To this end, we scale the spin labels by an overall constant  $\lambda$ , *i.e.*  $j_i \mapsto \lambda k_i$  and write (22) as

$$f(\hat{n}_i) = \frac{1}{2\pi^2} \sum_{\eta=\pm} \int_{B_\eta} \frac{d^3 \vec{p}}{\sqrt{1 - \vec{p}^2}} e^{\lambda S(\vec{p})}, \quad S(\vec{p}) := \sum_i 2k_i \ln (p_\eta + i \vec{p} \cdot \hat{n}_i). \quad (23)$$

Notice that the real part of  $S$  is negative. When the variable  $\lambda$  is taken to infinity, the integral can be approximated computing the saddle point expansion and evaluating the Gaussian integral on the maxima of  $S$ .<sup>2</sup> It is immediate to see that the norm of  $S$  is maximized by  $\vec{p} = 0$ , corresponding to  $h = 1$ , but the phase requires more attention. The saddle points of  $S(\vec{p})$  on  $B_\eta$  satisfy

$$\nabla S = \sum_i 2k_i \frac{(\vec{p} \cdot \hat{n}_i) \hat{n}_i - \vec{p}}{p_\eta^2 + (\vec{p} \cdot \hat{n}_i)^2} + i \frac{1}{p_\eta} \sum_i 2k_i \frac{(\vec{p} \cdot \hat{n}_i) \vec{p} + p_\eta^2 \hat{n}_i}{p_\eta^2 + (\vec{p} \cdot \hat{n}_i)^2} = 0. \quad (24)$$

A solution of this set of six real equations can be found taking the scalar product of the real part with  $\vec{p}$ , giving

$$\sum_i k_i \left( 1 - \frac{1}{p_\eta^2 + (\vec{p} \cdot \hat{n}_i)^2} \right) = 0.$$

Since  $0 \leq p_\eta^2 + (\vec{p} \cdot \hat{n}_i)^2 \leq 1$  and  $k_i > 0$  for all  $i$ 's, this implies that  $p_\eta^2 + (\vec{p} \cdot \hat{n}_i)^2 = 1$  for all  $i$ , namely  $\vec{p}^2 = (\vec{p} \cdot \hat{n}_i)^2$ .

This leaves us with two cases:

- Either there exists (at least) two non-collinear vectors,  $\hat{n}_i \neq \pm \hat{n}_j$ , then the latter equality forces  $\vec{p} = 0$  and the imaginary part of (24) simply reads  $\sum_i k_i \hat{n}_i = 0$ .
- Or all the  $\hat{n}_i$  are equal to the same unit vector  $\hat{n}$  up to a sign, then a little work on the imaginary part of (24) leads us to the same constraint  $\sum_i k_i \hat{n}_i = 0$  but leaves no constraint on the vector  $\vec{p}$ .

In both cases, we see that we have derived the closure condition (11) from the saddle point analysis in the large spin limit  $\lambda \rightarrow \infty$ . Numerical investigations show that there are no other solutions to (24), and that there are no saddle points if the closure condition is not satisfied. Which as we show below means that as  $\lambda$  increases the norm (15) is exponentially smaller for non-closed configurations, and thus correlations on spin networks in the large spin regime will be dominated by those intertwiners satisfying the closure condition and thus describing a classical geometry.

Let us start by the non-degenerate generic situation with non-collinear  $\hat{n}_i$ 's. Then  $S(0) = 0$  and the Hessian matrix of the second derivatives at the two (one for each three-ball) fixed points  $\vec{p} = 0$  is a sum of projectors  $P_{ab}^i = \left( \delta_{ab} - (\hat{n}_i)_a (\hat{n}_i)_b \right)$  orthogonal to the unit vectors  $\hat{n}_i$ ,

$$H_{ab} \equiv -\frac{1}{2} \frac{\partial^2}{\partial p_a \partial p_b} \Big|_{p=0} = \sum_i k_i P_{ab}^i. \quad (25)$$

Notice that this is independent of  $\eta$ , thus both saddle points give equal contributions. Next, the property  $\sum_{i,j} k_i k_j (n_i \cdot n_j)^2 < \sum_{i,j} k_i k_j$  guarantees that the eigenvalues of  $H_{ab}$

---

<sup>2</sup>Let us point out that the measure divergence at  $|p| = 1$  does not contribute at all to the leading order behaviour of the norm  $f(\hat{n}_i)$  unlike the case of the asymptotics of the 6j and 10j symbols [10]. Indeed, the divergence in  $\frac{1}{\sqrt{1-\vec{p}^2}}$  is still integrable and does not lead to a divergent integral.

are all positive. Therefore the Gaussian integral on the real line converges and we can straightforwardly compute the saddle point approximation,

$$f(\hat{n}_i) = \frac{1}{\pi^2} \int d^3 \vec{p} e^{-\lambda H_{ab} p_a p_b} = \frac{1}{\sqrt{\pi}} \frac{1}{\lambda^{3/2} \sqrt{\det H}}. \quad (26)$$

We can compute  $\det H$  explicitly in terms of the labels  $k_i$  and normals  $\hat{n}_i$ :

$$\det H = \frac{K}{2} \sum_{i,j} k_i k_j |\hat{n}_i \wedge \hat{n}_j|^2 - \frac{1}{6} \sum_{i,j,k} k_i k_j k_k |\hat{n}_i \cdot (\hat{n}_j \wedge \hat{n}_k)|^2,$$

with  $K = \sum_i k_i$ . When the closure constraint is satisfied, i.e.  $\sum_i k_i \hat{n}_i = 0$ , the quadratic term is a function of the (squared) area of the internal parallelograms while the cubic term relates to the (squared) volume of the tetrahedron. From this point of view, the determinant  $\det H$  measures the shape of the tetrahedron at fixed triangle area  $k_i$ .

The result (26) has been numerically confirmed for various closed configurations and different values of  $V$ . As an example, a plot is reported in Appendix D, which shows explicitly how accurate the approximation is, even for very small spins. In particular, we have one digit of accuracy from the beginning, and three digits at spins of order 100. We conclude that the norm of coherent intertwiners satisfying the closure condition scales as  $\lambda^{-3/2}$  in the large spin limit.

### 3.3 Degenerate configurations

Let us now look at the case where all the  $\hat{n}_i$ 's are collinear. Without loss of generality, we can take all the  $\hat{n}_i$ 's aligned with the  $z$  axis, namely  $\hat{n}_i = \eta_i \hat{z}$ ,  $\eta_i = \pm 1$ . Let us also define  $j^\pm = \sum_{i|\eta_i=\pm 1} j_i$ . One can easily convince himself that<sup>3</sup>  $f(\eta_i \hat{z}) \equiv 0$  unless  $\prod_i \eta_i = 1$  and  $j^+ = j^- \equiv \frac{V}{2} \lambda$ . Then, (20) reads  $(\cos \gamma + \eta_i \sin \gamma u_z)^{2j_i}$ . We take the conventional parametrization  $\mathcal{S}^2 \ni \hat{u} = (\cos \alpha \sin \beta, \sin \alpha \sin \beta, \cos \beta)$ , with normalized measure  $d^2 \hat{u} = \frac{1}{4\pi} d\alpha d\beta \sin \beta$ . We see that the  $\alpha$  angle drops out, and the integral is simply

$$\frac{1}{\pi} \int_0^\pi d\beta d\gamma \sin \beta \sin^2 \gamma (1 - \sin^2 \beta \sin^2 \gamma)^{V\lambda}. \quad (27)$$

This integral can be exactly evaluated as shown in the Appendix C, and the result is  $(V\lambda + 1)^{-1}$ .

We conclude that

$$f(\lambda, \eta_i \hat{z}) = \begin{cases} \frac{1}{V\lambda+1} & \text{if } \prod_i \eta_i = 1, j^+ = j^- \equiv \frac{V}{2} \lambda, \\ 0 & \text{otherwise.} \end{cases} \quad (28)$$

Notice that the degenerate configurations scale as  $\lambda^{-1}$ , whereas the closed ones scale as  $\lambda^{-3/2}$ . For  $\lambda \mapsto \infty$ , the degenerate configurations dominate as  $\sqrt{\lambda}$ . However, in the

---

<sup>3</sup>It suffices to decompose the state as in (14) and recall the conditions for a tensor product of states to admit singlet irreps.

partition function (4) they have zero measure, thus we do not expect them to affect the dynamics in a relevant way. Furthermore these degenerate configurations are also present in BC, and they do not enter the computation of physically relevant quantities, as conjectured in [11] and shown in [12].

### 3.4 Non-closed configurations

For configurations such that  $\vec{N} \neq 0$ , numerical simulations show that there are no saddle points, but the integrand in (22) is still maximized at  $\vec{p} = 0$ . For notational consistency, let us also rescale  $\vec{N} \mapsto \lambda \vec{N}$ . The expansion of  $S$  in (23) around  $\vec{p} = 0$  reads

$$S(\vec{p}) = 2i \vec{N} \cdot \vec{p} - H_{ab} p_a p_b + o(p^3). \quad (29)$$

If we approximate the integral using this expansion for the exponent, we see the presence of a phase term coming from the linear term in (29). This phase term dumps the integral exponentially. In fact, a simple calculation gives

$$f(\hat{n}_i) = \frac{1}{\pi^2} \int d^3 \vec{p} e^{i2\lambda \vec{N} \cdot \vec{p} - \lambda H_{ab} p_a p_b} = \frac{1}{\sqrt{\pi}} \frac{1}{\lambda^{3/2} \sqrt{\det H}} \left( e^{-\vec{N} \cdot H^{-1} \vec{N}} \right)^\lambda. \quad (30)$$

This result is again supported by numerical simulations for various non-closed configurations and different values of  $V$  (see Appendix D). As  $\vec{N} \cdot H^{-1} \vec{N} > 0$ , the norm of non-closed configurations is exponentially smaller than the closed ones.

We do not have a simple explicit expression for the inverse Hessian  $H^{-1}$ , but we can easily write it as a power series. Notice that  $H$  in (25) reads as  $K(\mathbb{1} - \Sigma)$  with  $K = \sum_i k_i$  and  $\Sigma_{ab} = \sum_i (k_i/K) \hat{n}_i^a \hat{n}_i^b$ . As the norm of  $\Sigma_{ab}$  is smaller than 1, the inverse series for  $H^{-1}$  converges (except in the degenerate configurations where some of the  $\hat{n}_i$  are collinear):

$$H^{-1} = \frac{1}{K} [\mathbb{1} + \Sigma + \Sigma^2 + \dots] = \frac{1}{K} \left[ \mathbb{1} + \sum_i \frac{k_i}{K} \hat{n}_i^a \hat{n}_i^b + \sum_{i,j} \frac{k_i k_j}{K^2} (\hat{n}_i \cdot \hat{n}_j) \hat{n}_i^a \hat{n}_j^b + \dots \right].$$

This allows us to express the exponent of (30) in terms of the matrix  $G_{ij} \equiv \frac{\sqrt{k_i k_j}}{K} (\hat{n}_i \cdot \hat{n}_j)$ ,

$$\begin{aligned} N \cdot H^{-1} N &= \frac{1}{K} \sum_{i,j} k_i k_j (\hat{n}_i \cdot \hat{n}_j) + \frac{1}{K^2} \sum_{i,j,k} k_i k_j k_k (\hat{n}_i \cdot \hat{n}_j) (\hat{n}_j \cdot \hat{n}_k) + \dots \\ &= \sqrt{k_i} (G + G^2 + G^3 + \dots)_{ij} \sqrt{k_j}. \end{aligned}$$

Notice that  $G_{ij}$  is a  $V \times V$  Gram matrix of scalar products of unit vectors. For  $V$  greater than 3, the vectors  $\hat{n}_i$  are not linearly independent and  $\det G_{ij} = 0$ . Nevertheless the series  $G + G^2 + G^3 + \dots$  can be re-summed as  $G(\mathbb{1} - G)^{-1}$ . Thus it appears that the speed of convergence of the intertwiner norm in this non-closed case is directly related to the eigenvalues of the Gram matrix  $G$ . More precisely, estimating its smallest and largest eigenvalues (both between 0 and 1) would allow to bound the convergence speed of the norm as  $\lambda$  goes to infinity.

## 4 Four-valent case: the coherent tetrahedron

Above we have constructed coherent intertwiners for nodes of generic valence. The 4-valent case, whose dual geometric picture is a tetrahedron, is of particular interest as it enters the construction of vertex amplitudes for spinfoam models. In this Section, we study how the coherent tetrahedron can be decomposed in the conventional basis of virtual links, which we fix by choosing to add  $\vec{J}_1$  and  $\vec{J}_2$  first.

The coefficients entering (14) can be studied with the same techniques used for the norms. Introducing the shorthand notation  $|i\rangle \equiv |j_i, \hat{n}_i\rangle$ , in the 4-valent case we have

$$|\langle j_1 \dots j_4, j_{12} | \underline{j}, \underline{\hat{n}} \rangle_0|^2 = \int dh \int dg d_{j_{12}} \chi^{(j_{12})}(g) \langle 12 | hg | 12 \rangle \langle 34 | h | 34 \rangle. \quad (31)$$

As it can be verified directly,  $d_{j_{12}} \chi^{(j_{12})}(g)$  projects on the intertwiner state  $|j_1 \dots j_4, j_{12}\rangle$ . To study the asymptotics, it is convenient to introduce an auxiliary unit vector  $\hat{n}$ , writing the character in the basis of coherent states,

$$\chi^{(j_{12})}(g) = d_{j_{12}} \int d^2 \hat{n} \langle j_{12}, \hat{n} | g | j_{12}, \hat{n} \rangle. \quad (32)$$

As in the previous Section, we parametrize the group elements as  $h = p_\eta + i\vec{p} \cdot \vec{\sigma}$ ,  $g = q_{\eta'} + i\vec{q} \cdot \vec{\sigma}$ . We have

$$gh = p_\eta q_{\eta'} - \vec{p} \cdot \vec{q} + i \left( p_\eta \vec{q} + q_{\eta'} \vec{p} - \vec{p} \wedge \vec{q} \right) \cdot \vec{\sigma}. \quad (33)$$

Using this and (20), and rescaling again  $j_i \mapsto \lambda k_i$ , we rewrite (31) as

$$|\langle j_1 \dots j_4, j_{12} | \underline{j}, \underline{\hat{n}} \rangle_0|^2 = \frac{d_{j_{12}}^2}{(2\pi^2)^2} \sum_{\eta, \eta' = \pm} \int_{B_\eta} \frac{d^3 \vec{p}}{\sqrt{1 - \vec{p}^2}} \int_{B_{\eta'}} \frac{d^3 \vec{q}}{\sqrt{1 - \vec{q}^2}} \int d^2 \hat{n} e^{\lambda S(\vec{p}, \vec{q})} \quad (34)$$

with

$$\begin{aligned} e^{S(\vec{p}, \vec{q})} &= (q_{\eta'} + i\vec{q} \cdot \hat{n})^{2k_{12}} \prod_{i=1}^2 \left( p_\eta q_{\eta'} - \vec{p} \cdot \vec{q} + i (p_\eta \vec{q} + q_{\eta'} \vec{p} - \vec{p} \wedge \vec{q}) \cdot \hat{n}_i \right)^{2k_i} \\ &\times \prod_{i=3}^4 (p_\eta + i\vec{p} \cdot \hat{n}_i)^{2k_i}. \end{aligned} \quad (35)$$

From the analysis of the previous Sections, we expect the asymptotics of these coefficients to be dominated by  $g$  and  $h$  close to the identity. Expanding  $S$  around  $\vec{p} = \vec{q} = 0$  and denoting  $\underline{r} = (\vec{p}, \vec{q})$ , we have

$$S(\underline{r}) = 2i \tilde{N} \cdot \underline{r} - \underline{r} \cdot \tilde{H} \underline{r} + o(r^3), \quad (36)$$

where  $\tilde{N}$  is the following 6-dimensional vector,

$$\tilde{N} = \begin{pmatrix} \vec{N} \\ k_1 \hat{n}_1 + k_2 \hat{n}_2 + k_{12} \hat{n} \end{pmatrix}. \quad (37)$$

The Hessian matrix has the following structure,

$$\tilde{H} = \begin{pmatrix} H & F \\ F^T & H' \end{pmatrix}, \quad (38)$$

with  $H$  the same as in (25), and

$$F_{ab} = k_1 P_{ab}^1 + k_2 P_{ab}^2 - i \eta \eta' \epsilon_{abc} \left( k_1 (\hat{n}_1)_c + k_2 (\hat{n}_2)_c \right), \quad (39)$$

$$H'_{ab} = k_1 P_{ab}^1 + k_2 P_{ab}^2 + k_{12} P_{ab}. \quad (40)$$

The antisymmetric part of  $F$  comes from the  $\vec{p} \wedge \vec{q}$  term in (33), so from the non-abelian nature of  $SU(2)$ . Notice that the only imaginary term in  $\tilde{H}$  is proportional to  $\eta \eta'$ , thus when we perform the sums in the Gaussian approximation, we are simply going to get (four times) the real part of a single Gaussian integration.

The asymptotics are given by

$$|\langle j_1 \dots j_4, j_{12} | \underline{j}, \underline{\hat{n}} \rangle_0|^2 \simeq \frac{d_j^2}{\pi \lambda^3} \sum_{\eta, \eta' = \pm} \int d^2 \hat{n} \frac{1}{\sqrt{\det \tilde{H}}} \left( e^{-\tilde{N} \cdot \tilde{H}^{-1} \tilde{N}} \right)^\lambda, \quad (41)$$

where  $\det \tilde{H}$  can be expressed in term of  $3 \times 3$  determinants as  $\det H \det(G - F^T H^{-1} F)$ . This integral can be studied numerically. For fixed  $j_i$ ,  $\hat{n}_i$ , it represents the probability of the eigenstate  $j_{12}$  as a function of the  $\hat{n}_i$ 's. For closed configurations, we expect this to be a Gaussian peaked on the semiclassical value computed from the  $\hat{n}_i$ 's. Let us consider for simplicity the equilateral case. In this case, we expect  $j_{12}$  to be peaked around  $\bar{j}$  such that  $\bar{j}(\bar{j} + 1) = \langle (\vec{J}_1 + \vec{J}_2)^2 \rangle = 2j_0(\frac{2}{3}j_0 + 1)$ , which gives  $\bar{j} = \sqrt{2j_0(\frac{2}{3}j_0 + 1)} + \frac{1}{4} - \frac{1}{2}$ . As we show in Fig.1, for large spin (41) is indeed approximated by the Gaussian

$$p(j_{12}) = N(j_0) \exp \left\{ -\frac{(j_{12} - \bar{j})^2}{\sigma} \right\}, \quad (42)$$

where  $N(j_0)$  is the normalization. Confronted with the numerics, we fix  $\sigma = j_0/2$ . This semiclassical property is manifestly preserved by changing the pairing, namely the choice of basis. For any choice of  $j_{ik}$  the probability (41) is peaked on  $j_{ik}(j_{ik} + 1) \sim (j_i \hat{n}_i + j_k \hat{n}_k)^2$  with vanishing relative uncertainty.<sup>4</sup>

Analogous results hold for arbitrary closed configurations. This shows in a concrete way in which sense  $|\underline{j}, \underline{\hat{n}}\rangle_0$  represents a semiclassical state for a quantum tetrahedron, and more in general for a  $V$ -simplex dual to a node of valence  $V$ .

At this point, it is useful to compare our construction of the semiclassical tetrahedron with the one introduced in [6]. Both states have the property that for any  $i$  and  $k$ ,  $\langle \vec{J}_i \cdot \vec{J}_k \rangle$

---

<sup>4</sup>An alternative definition of coherent states, considered in [13], is to require the minimization of the uncertainty  $\Delta \vec{J}_i \cdot \vec{J}_k \Delta \vec{J}_i \cdot \vec{J}_l \geq \frac{1}{2} |\langle [\Delta \vec{J}_i \cdot \vec{J}_k, \Delta \vec{J}_i \cdot \vec{J}_l] \rangle| \equiv \frac{1}{2} |\langle \epsilon_{abc} J_i^a J_k^b J_l^c \rangle| \sim O(j^3)$ . The states constructed here do not strictly minimize this, even if they do satisfy the non trivial condition  $\Delta \vec{J}_i \cdot \vec{J}_k \Delta \vec{J}_i \cdot \vec{J}_l \sim O(j^3)$  which guarantees the vanishing relative uncertainties.

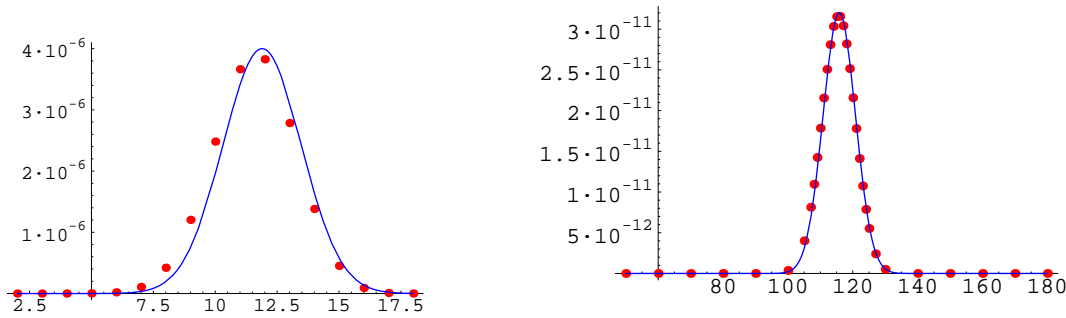


Figure 1: Plots of (41) for the equilateral configuration  $j_i = j_0 \forall i$ . The dots represent the exact numerical evaluation, whereas the line is the Gaussian (42). The left panel shows the case  $j_0 = 10$ , whereas the right panel shows the case  $j_0 = 100$ . In the small spin case, the Gaussian approximation is already capturing the right behavior, and it becomes very accurate in the large spin case.

is peaked around a given semiclassical value with vanishing relative uncertainty in the large spin limit. The uncertainties are slightly different, as can be seen by direct comparison in the equilateral case. From equation (41) of [6] (with the appropriate redefinition of  $j_0$ ) we read  $\sigma = 4j_0/3\sqrt{3}$  which is roughly one and a half times the spread of (42). The main advantage of the states introduced here lies in the fact that they allow the construction of a wider framework. The construction in [6] is only valid for a tetrahedron, and tailored to studying the large spin limit only. The framework considered here, on the other hand, applies to any  $V$ -simplex, and it is well-defined for any spin. In particular, the key feature of the coherent intertwiners considered here is that they provided an overcomplete basis in  $\mathcal{H}_0$ , which makes them useful to study the dynamics, as we described in Section 2.

## 5 Towards the quantum gravity amplitude

Let us finally discuss how the coherent state technology presented here can be used to define the dynamics of quantum GR, starting from the spinfoam model (4). Spinfoam quantization of GR usually relies on reformulating GR as a constrained BF theory with an action of the following type [14, 15, 16],

$$S_{\text{GR}}(B_{\mu\nu}, \omega_\mu) = \int \text{Tr } B \wedge F(\omega) + \mathcal{C}(B_{\mu\nu}). \quad (43)$$

$\omega_\mu$  is a connection valued on a given Lie algebra (for euclidean signature,  $\mathfrak{su}(2)$  or  $\mathfrak{spin}(4)$ ), and  $B_{\mu\nu}$  is a bivector field (or two-form) with values in the same Lie algebra. The term  $\mathcal{C}(B)$  includes polynomial constraints, reducing topological BF to GR.<sup>5</sup> Typically, it gives

---

<sup>5</sup>The logic of this reduction is the following. The initial BF action describes a topological theory with no local degree of freedom, with the field  $B$  a Lagrange multiplier enforcing that the connection is flat,  $F(\omega) = 0$ . The term  $\mathcal{C}(B)$  then constrains the Lagrange multiplier, thus enlarging the phase space. It breaks the topological invariance (translation symmetry of  $B$ ) and introduces non-trivial local degrees of freedom.

the set of second class constraints expressing  $B$  in terms of the tetrad field (or vierbein) and leading to GR in the first order formalism (for a detailed canonical analysis of (43), see [17]).

The BF theory can be quantized as described in Section 2, discretizing the spacetime manifold with a Regge triangulation (or more generally a cellular decomposition), and then evaluating the partition function (2), where the variables are the representations  $j_t$  and intertwiners  $i_\tau$ . The natural extension of this procedure to quantize GR with action (43) would be to discretize the constraints  $\mathcal{C}(B)$  and include them in the computation of the discretized path integral (see e.g. [18, 19]). Nevertheless, on the grounds of geometric quantization (see e.g. [2]), one usually shortcuts this computation and directly attempts to translate the discretized constraints  $\mathcal{C}(B)$  as constraints on the variables  $j_t$  and  $i_\tau$  by assuming that the variables  $B$  are represented in the spinfoam as the generators of the considered Lie group, as in (7) for  $SU(2)$ . This procedure is usually referred to as imposing the constraints at the quantum level, and it leads to a unique choice of intertwiner and to the Barrett-Crane model [2, 20]. However, the quantum constraints obtained in this way are fairly strong, and a number of authors have raised various doubts on this procedure, such as: the rewriting of the constraints in purely algebraic terms (representations and intertwiners) partially hides their geometric meaning, and thus the interpretation of the model; the unique intertwiner does not seem to be compatible with the data on the boundary spin network as given in LQG; more crucially, the quantum constraints do not commute with each other and generate (by commutator) higher order constraints which do not seem to have any classical equivalent.

A plausible explanation of these difficulties is that the BC model imposes the constraints too strongly, and thus does not have enough degrees of freedom to describe quantum GR. Then a way out would be to loosen the implementation of the constraints, by requiring them to hold only on average (vanishing expectation value) with minimal uncertainty. This seems the natural procedure when dealing with non-commuting constraints.<sup>6</sup> It has been suggested for instance in [18], where both possibilities are discussed, (i) to impose the constraints exactly by inserting the  $\delta$ -distribution  $\delta(\mathcal{C}(B))$  in the path integral, or (ii) to regularize the  $\delta$ -distribution by inserting its Gaussian approximation  $\exp(-\mathcal{C}(B)^2/\xi^2)$ , with  $\xi$  a free parameter. Notice that the Gaussian insertion amounts to impose the constraints approximatively. More precisely, since the  $B$  field represents the geometry and large values of  $B$  corresponds to large (length) scales, using the Gaussian means imposing the constraints at the semiclassical level while allowing slight deviations at smaller scales.

In the same spirit, here we argue that the partition function (4) for the quantum BF theory in terms of coherent states offers a natural way to impose the constraints on average. The key is that the partition function (4) provides a quantization of BF theory where the  $B$  field is represented not through generators of the group, but as representation and intertwiner labels, such as  $j_t$  and  $\hat{n}_t$  (see (6) or (8)). This representation allows to write directly the constraints  $\mathcal{C}(B)$  as a sum of local contributions  $\mathcal{C}_\sigma(j_t \hat{n}_{t,\tau})$ , in terms of the

---

<sup>6</sup>A possible strategy to impose strongly second class constraints is discussed in [21].

dynamical variables and with a clear geometric interpretation. In particular, the semiclassical dynamics becomes transparent. As we understand from the analysis reported in the previous Sections, the vertex is dominated in the large spin limit by semiclassical states satisfying the closure condition for each tetrahedron and the relation (10) between adjacent tetrahedra in the same 4-simplex. On these states the variables  $j_t$  and  $\hat{n}_t$  give classical values with an (almost minimal) uncertainty decreasing as the  $j_t$ 's increase. Therefore, imposing  $\mathcal{C}_\sigma(j_t \hat{n}_{t,\tau}) = 0$  amounts to impose the classical constraints only on average with a small uncertainty vanishing in the large spin limit, namely semiclassically. If we use the  $j_t$ 's and  $\hat{n}_t$ 's to construct a Regge geometry, we expect that the role of the constraints is to generate deficit angles when we glue together various 4-simplices, thus allowing the geometry to be curved. We postpone the precise analysis of the implementation of the constraints for further work.

## 6 Conclusions

The standard intertwiner basis which leads to BF theory with the vertex amplitude given by the  $\{15j\}$  symbol does not appear to be the most suitable one to study the semiclassical geometry of BF theory. Furthermore, it makes it hard to understand the quantum structure of the constraints reducing BF to GR, and possibly hides the correct way to implement them.

Here we considered a basis constructed out of  $SU(2)$  coherent states. We defined non-normalized coherent intertwiners, and studied their norm as a function of the geometric configuration described. For each configuration, the norm is an integral over  $SU(2)$  that can be solved exactly as described in the Appendix. Yet a saddle point evaluation of the leading order of this integral in the large spin limit proves a very accurate approximation even for small spins, and shows very neatly that the norm is exponentially maximized by the states admitting a semiclassical interpretation, namely the ones whose quantum numbers can be interpreted as vectors  $j_i \hat{n}_i$  describing the classical discrete geometry of a  $V$ -simplex. Thanks to this crucial result, the semiclassical states will dominate the evaluation of quantum correlations.

Using these coherent intertwiners we rewrote the BF partition function with a new vertex amplitude, given in (5), where the discrete  $B_t(\tau)$  variables are interpreted in terms of the vectors  $j_t \hat{n}_{t,\tau}$ , thus retaining the original vectorial nature of the  $B$  field. We expect this reformulation of the BF spinfoam amplitudes to improve the geometric interpretation of the theory and in particular our understanding of what should be the proper way to implement the constraints reducing it to GR.

We hope that the developments presented here will contribute to the promising recent advances in understanding the low energy limit of LQG, such as the ones on the graviton propagator [3, 11, 12, 22], on the emergence of effective actions for matter [23], or on applications to cosmology [24] and black hole physics [25].

## Acknowledgments

Research at Perimeter Institute for Theoretical Physics is supported in part by the Government of Canada through NSERC and by the Province of Ontario through MRI.

## A Coherent States for $SU(2)$ : a brief review

$SU(2)$  coherent states minimize the ( $SU(2)$  invariant) uncertainty  $\Delta \equiv |\langle \vec{J}^2 \rangle - \langle \vec{J} \rangle^2|$  in the direction of the angular momentum [27]. A simple calculation shows that on a basis state  $|j, m\rangle$  the uncertainty  $\Delta(j, m) = j(j+1) - m^2$  is minimal when  $m = j$ . The maximal weight vectors  $|j, j\rangle$  are thus coherent states for arbitrary choice of spin  $j$  and angular momentum axis  $J_z$ . Starting from the highest weight, an infinite set of coherent states on the sphere  $SU(2)/U(1) \sim S^2$  are constructed through the group action,  $|j, \hat{n}\rangle = g(\hat{n})|j, j\rangle$ , where  $\hat{n}$  is a unit vector defining a direction on the sphere  $S^2$  and  $g(\hat{n})$  a  $SU(2)$  group element rotating the direction  $\hat{z} \equiv (0, 0, 1)$  into the direction  $\hat{n}$ . Explicitly, taking  $\hat{n} = (\sin \theta \cos \phi, \sin \theta \sin \phi, \cos \theta)$ , we choose  $g(\hat{n}) \equiv \exp\{i\theta \hat{m} \cdot \vec{J}\}$  where  $\hat{m} \equiv (\sin \phi, -\cos \phi, 0)$  is a unit vector orthogonal to both the directions  $\hat{z}$  and  $\hat{n}$ . Just as  $|j, j\rangle$  has direction  $z$  with minimal uncertainty,  $|j, \hat{n}\rangle$  has direction  $\hat{n}$  with minimal uncertainty, as can be verified explicitly using the formula reported in the next Appendix.

A coherent state can be decomposed in the usual basis as

$$|j, \hat{n}\rangle = \sum_{m=-j}^j a_m(\hat{n})|j, m\rangle, \quad (44)$$

where

$$a_m(\hat{n}) = \sqrt{\frac{(2j)!}{(j-m)!(j+m)!}} \frac{\zeta^{j-m}}{(1+|\zeta|^2)^j}, \quad \zeta = \tan \frac{\theta}{2} e^{-i\phi}.$$

These states are normalized but not orthogonal, the scalar product between two of them being

$$\langle j, \hat{n}_1 | j, \hat{n}_2 \rangle = \left( \frac{1 + \hat{n}_1 \cdot \hat{n}_2}{2} \right)^j e^{ijA(z, \hat{n}_1, \hat{n}_2)}, \quad A(z, \hat{n}_1, \hat{n}_2) = -\frac{i}{2} \ln \left( \frac{1 + \xi_1 \bar{\xi}_2}{1 + \bar{\xi}_1 \xi_2} \right).$$

Here  $\xi = \frac{\theta}{2} e^{-i\phi}$ . Notice that  $A$  is the area of the geodesic triangle on the sphere  $S^2$  by the north pole direction  $z$  and the two unit vectors  $\hat{n}_1$  and  $\hat{n}_2$ .

Consequently they provide an overcomplete basis for the irreps  $j$ , and the resolution of the identity can be written as  $\mathbb{1}_j = d_j \int d^2 \hat{n} |j, \hat{n}\rangle \langle j, \hat{n}|$ , with  $d^2 \hat{n}$  the normalized measure on  $S^2$ .

The explicit coefficients entering (14) can be found using (44) to decompose  $|\underline{j}, \underline{\hat{n}}\rangle_0$  into the conventional basis of  $\mathcal{H}_0$ ,

$$\mathcal{H}_0 \ni |\underline{j}, \underline{\hat{n}}\rangle_0 = \sum_{m_1 \dots m_V} \prod_{i=1}^V a_{m_i}(\hat{n}_i) \sum_{i_1 \dots i_{V-3}} C_{m_1 \dots m_V}^{i_1 \dots i_{V-3}} |j_1 \dots j_V, i_1 \dots i_{V-3}\rangle, \quad (45)$$

where we have introduced the (generalized) Clebsch-Gordan coefficients  $C_{m_1 \dots m_V}^{i_1 \dots i_{V-3}}$  (see [28]). These are defined<sup>7</sup> by the integration of irrep matrices,

$$\int dg \prod_{i=1}^V D_{m_i n_i}^{(j_i)}(g) = \sum_{i_1 \dots i_{V-3}} \overline{C_{m_1 \dots m_V}^{i_1 \dots i_{V-3}}} C_{n_1 \dots n_V}^{i_1 \dots i_{V-3}}. \quad (46)$$

Using the recoupling theory, these generalized coefficients can always be decomposed into sums of products of conventional (3-valent) Clebsch-Gordan coefficients.

From (45) we immediately read the coefficients entering (14).

## B Useful formulas

We report here the results used in Section 3. The calculations can be done using the explicit expression (44), however it is usually easier to exploit the fact that

$$\langle j, \hat{n} | J_a | j, \hat{n} \rangle = \langle j, j | J'_a | j, j \rangle$$

where  $J'_a = g(\hat{n})^{-1} J_a g(\hat{n})$  is the rotated generator.

We compute the following averages of the SU(2) generators on the coherent states:

$$\langle j, \hat{n} | J_a | j, \hat{n} \rangle = j n_a, \quad \langle j, \hat{n} | J_a^2 | j, \hat{n} \rangle = \frac{j}{2} + j(j - \frac{1}{2}) n_a^2. \quad (47)$$

From this it is easy to check that

$$\Delta^2 \equiv \langle j, \hat{n} | \vec{J}^2 | j, \hat{n} \rangle - \langle j, \hat{n} | \vec{J} | j, \hat{n} \rangle \langle j, \hat{n} | \vec{J} | j, \hat{n} \rangle = j.$$

Further calculations give

$$\langle j, \hat{n} | J_a J_b | j, \hat{n} \rangle = \frac{j}{2} (\delta_{ab} + i \epsilon_{abc} n_c) + j(j - \frac{1}{2}) n_a n_b,$$

$$\langle 12 | (\vec{J}_1 + \vec{J}_2)^2 | 12 \rangle = (j_1 \hat{n}_1 + j_2 \hat{n}_2)^2 + j_1 + j_2,$$

(here notice that the  $j_1 + j_2$  term comes from the uncertainty  $\Delta^2$  computed above), and

$$\begin{aligned} \langle 12 | (\vec{J}_1 + \vec{J}_2)^4 | 12 \rangle &= ((j_1 \hat{n}_1 + j_2 \hat{n}_2)^2 + j_1 + j_2)^2 + \\ &+ 2j_1 j_2 \left[ \left( j_1 + j_2 - \frac{1}{2} \right) \left( 1 - (\hat{n}_1 \cdot \hat{n}_2)^2 \right) + (1 - 3 \hat{n}_1 \cdot \hat{n}_2) \right]. \end{aligned}$$

Therefore the uncertainty  $\langle (\vec{J}_1 + \vec{J}_2)^4 \rangle - \langle (\vec{J}_1 + \vec{J}_2)^2 \rangle^2$  depends explicitly on the value of the angle  $\cos \theta_{12} = \hat{n}_1 \cdot \hat{n}_2$ . For large  $j_1, j_2$ , it is for aligned vectors and maximal for  $\hat{n}_1$  and  $\hat{n}_2$  orthogonal.

Proceeding as above, one can show (13) for any observable  $\hat{O}(\vec{J}_i)$ .

Let us now report other results used in the main body of the paper.

---

<sup>7</sup>Here we loosely use the term Clebsch-Gordan coefficients, to refer to invariant tensors. These can differ in phase and normalization from other definitions found in the literature.

- The matrix element entering the bivalent norm (18) can be computed directly using the conventional parametrization

$$g(\hat{n}_i) \equiv g(\theta_i, \hat{m}_i) = \cos \theta_i \mathbb{1} + i \sin \theta_i \hat{m}_i \cdot \vec{\sigma}, \quad (48)$$

we have

$$\begin{aligned} |\langle + | g_1^{-1} g_2 | - \rangle|^2 &= \cos^2 \theta_1 + \cos^2 \theta_2 - 2 \cos \theta_1 \cos \theta_2 (\cos \theta_1 \cos \theta_2 + \sin \theta_1 \sin \theta_2 \hat{m}_1 \cdot \hat{m}_2) = \\ &= \frac{1 - \hat{n}_1 \cdot \hat{n}_2}{2} = 1 - \frac{1}{4} (\hat{n}_1 + \hat{n}_2)^2. \end{aligned} \quad (49)$$

- In Section 3 we also made use of the adjoint action of the group on itself. Using (21) and (48), we have

$$g(\hat{n})^{-1} h g(\hat{n}) = \cos \gamma + i \sin \gamma \hat{u}' \cdot \vec{\sigma}, \quad \hat{u}' = g(\hat{n})^{-1} \hat{u}.$$

By definition  $g(\hat{n})$  rotates the north pole vector  $(0, 0, 1)$  to the direction  $\hat{n}$ , thus  $(\hat{u}')_3 = (g(\hat{n})^{-1} \hat{u})_3 = \hat{u} \cdot \hat{n}$ , as can be explicitly checked writing the components of the rotated vector  $\hat{u}'$ :

$$\hat{u}' = \cos \theta \hat{u} - \sin \theta \hat{u} \wedge \hat{m} + 2 \sin^2 \frac{\theta}{2} (\hat{u} \cdot \hat{m}) \hat{m},$$

$$(\hat{u}')_3 = \cos \theta \hat{u}_3 - \sin \theta (\hat{u} \wedge \hat{m})_3 = \cos \theta \hat{u}_3 + \sin \theta (\hat{u}_1 \cos \phi + \hat{u}_2 \sin \phi) = \hat{u} \cdot \hat{n}.$$

From this we immediately derive (20).

- A crucial result concerns the extension of (13) to expectation values in  $\mathcal{H}_0$ . To prove this, one can compute

$$\langle j, \hat{n} | h \vec{J} | j, \hat{n} \rangle = j [\cos \gamma \hat{n} + i \sin \gamma \hat{u} + \sin \gamma \hat{u} \wedge \hat{n}] (\cos \gamma + i \sin \gamma \hat{u} \cdot \hat{n})^{2j-1}.$$

As we see, the presence of the group element  $h$  complicates the expectation values of the  $SU(2)$  generators (compare the above with (47)). However, we know from the analysis in Section 3 that the integration over  $h$  peaks the group elements on the identity  $\gamma = 0$  in the large spin limit, thus

$$\int dh \langle j, \hat{n} | h \vec{J} | j, \hat{n} \rangle \simeq j \hat{n},$$

and all the results reported above extend naturally to  $\mathcal{H}_0$  in the large spin limit.

## C Evaluating the norm using spherical integrals

In Section 3 we wrote the norm (22) using  $\vec{p}$  to parametrize  $SU(2)$ . This choice was convenient to study the saddle point approximation. On the other hand, to evaluate the norm exactly, it is more useful the standard parametrization (21) in terms of a rotation angle  $\gamma$  and its rotation axis  $\hat{u}$ ,

$$f(\hat{n}_i) = \int dh \langle j_i, \hat{n}_i | h^{\otimes V} | j_i, \hat{n}_i \rangle = \frac{2}{\pi} \int_0^\pi d\gamma \sin^2 \gamma \int_{S^2} d^2 \hat{u} \prod_{i=1}^V (\cos \gamma + i \sin \gamma \hat{u} \cdot \hat{n}_i)^{2j_i}.$$

We can expand all the terms and deal separately with the integrals over  $\gamma$  and the spherical integrals over  $\hat{u}$ . Using the binomial expansion and  $J \equiv \sum_i j_i$ , the  $d\gamma$  integrals are of the following type,

$$\mathcal{I}(J, k) \equiv \frac{2}{\pi} \int d\gamma (\sin \gamma)^{2+2k} (\cos \gamma)^{2J-2k} = \frac{(2J)! (2k+1)!! (2J-2k-1)!!}{2^{2J} (J+1) (J!)^2 (2J-1)!!}, \quad (50)$$

with  $k \leq J$ .

The next step is to compute the spherical integrals. One can show that:

$$\begin{aligned} \int d^2 \hat{u} \prod_{i=1}^2 (\hat{u} \cdot \hat{n}_i) &= \frac{1}{3} \hat{n}_1 \cdot \hat{n}_2, \\ \int d^2 \hat{u} \prod_{i=1}^4 (\hat{u} \cdot \hat{n}_i) &= \frac{1}{3 \times 5} [(\hat{n}_1 \cdot \hat{n}_2)(\hat{n}_3 \cdot \hat{n}_4) + (\hat{n}_1 \cdot \hat{n}_3)(\hat{n}_2 \cdot \hat{n}_4) + (\hat{n}_1 \cdot \hat{n}_4)(\hat{n}_2 \cdot \hat{n}_3)]. \end{aligned}$$

This can be generalized to even polynomials of arbitrary high order in  $\hat{u}$ . A generic term  $\int \prod_i^{2N} (\hat{u} \cdot \hat{n}_i)$  will have a prefactor  $(2N+1)!!$  and a sum over the  $(N-1)!!$  possible pairings of the vectors  $\hat{n}_i$  with each other.

Using these formulas one can compute exactly the coherent intertwiner norm  $f(\hat{n}_i)$  as a finite sum of polynomials of the  $\hat{n}_i$ .

The situation is particularly simple in the degenerate case, when all the  $\hat{n}_i$  are aligned. In this case, discussed in Section 3.3, the spherical integrals are trivial, and we have to evaluate simply

$$\begin{aligned} f(N, \eta_i \hat{z}) &= \frac{1}{\pi} \int d\beta d\gamma \sin \beta \sin^2 \gamma (1 - \sin^2 \beta \sin^2 \gamma)^N = \\ &= \frac{1}{\pi} \sum_{k=0}^N (-1)^k \binom{N}{k} \int d\beta (\sin \beta)^{2k+1} \int d\gamma (\sin \gamma)^{2k+2} = \sum_{k=0}^N \frac{(-1)^k}{k+1} \binom{N}{k}, \end{aligned} \quad (51)$$

where in the last step we used

$$\int d\beta (\sin \beta)^{2k+1} = \sqrt{\pi} \frac{\Gamma(k + \frac{3}{2})}{\Gamma(k+2)}, \quad \int d\gamma (\sin \gamma)^{2k+2} = \sqrt{\pi} \frac{\Gamma(k+1)}{\Gamma(k + \frac{3}{2})}.$$

This sum in (51) can be straightforwardly evaluated with the substitution  $t = s + 1$ , to obtain

$$f(N, \eta_i \hat{z}) = \frac{1}{N+1} \sum_{t=1}^{N+1} \frac{(-1)^{t-1} (N+1)!}{t! (N+1-t)!} = -\frac{1}{N+1} \left( (1-1)^{N+1} - 1 \right) \equiv \frac{1}{N+1}. \quad (52)$$

This result was used to evaluate (27).

## D Numerics

All the calculations of this paper have been supported by numerical simulations, performed with Mathematica<sup>TM</sup>. In this Appendix we report some examples to illustrate the numerical support to the saddle point analysis of Sections 3.2 and 3.4.

The first thing we show is the absence of saddle points when the closure is not satisfied. Consider the integrand in (22), with the parametrization (21) where  $\hat{u} = (\cos \alpha \sin \beta, \sin \alpha \sin \beta, \cos \beta)$ . To give a clear picture of the integrand, we fix an arbitrary value of  $\alpha$  and show a 3d plot in only  $\beta$  and  $\gamma$ . We choose the simplest case, the equilateral tetrahedron ( $V = 4$ ) with  $j_i = 100 \forall i$ . This is shown on the left panel of Fig.2. It is clearly visible that  $\gamma = 0$  is a saddle point (the degeneracy in  $\beta$  is an artifact of the polar coordinates for  $\mathcal{S}^3$ ), and that the integrand is quickly suppressed away from it. On the right panel, we have again  $V = 4$ , but this time we picked a random non closed configuration, with the four different spins still of order 100, but not equal. First of all, one can notice that even if  $\gamma = 0$  still maximizes the integrand, it is not anymore a saddle point. Second, notice that the integrand has now also negative values, which contribute to dump the integral in this non closed case.

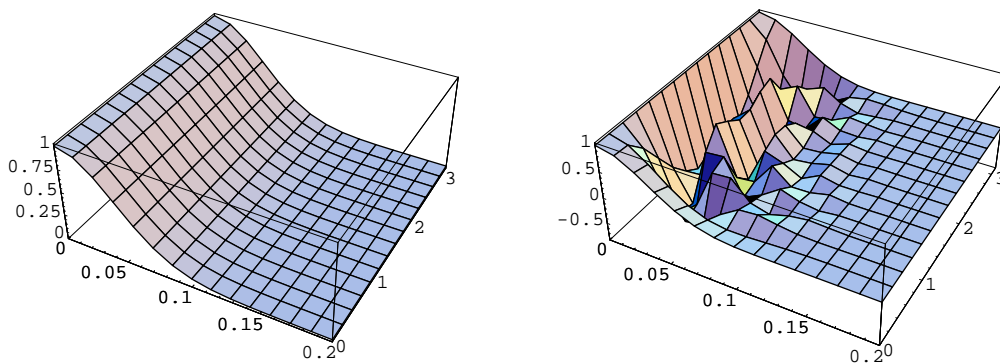


Figure 2: The real part of the integrand for  $V = 4$  as a function of  $\gamma \in [0, 0.2]$  (symmetric at  $\pi/2$ ) and  $\beta \in [0, \pi]$ , for fixed  $\alpha$ . Left panel: the equilateral case, at  $j_i = 100$  for all  $i$ . Right panel: a generic open configuration, with different spins but all of order 100.

Next, we consider the Gaussian evaluation of the norm. In Fig.3 we compare the exact numerical evaluations of (22) with the analytic calculations. On the left panel, we consider a closed configuration, for simplicity given by the equilateral tetrahedron, namely

$V = 4$  and  $j_i = j \forall i$ . The dots represent the numerical evaluations for different values of  $j$ , whereas the line is the analytic result (26). As one can see, the agreement is very good also at small spins. By direct reading of the numerics, one sees that the analytic approximation matches to one digit the exact result already at  $j \sim 1$ , and that at  $j \sim 100$  the matching is to three digits. The situation is very similar for arbitrary configurations. On the right panel we consider a non closed configuration with  $j_i = j \forall i$ . The dots are again the numeric evaluations, and the line the analytic result (30). Notice that the agreement is still very good even at small spins. As expected, the norm is exponentially smaller than in the closed configuration. In the open case, the integral converges poorly, for this reason we have less points in the plot.

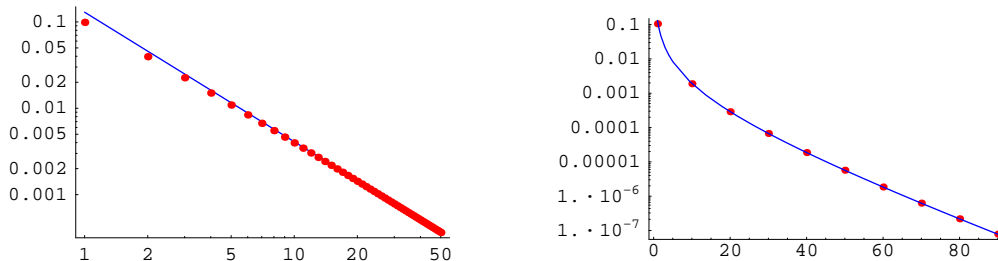


Figure 3: Bilogarithmic plots. *Left panel:* the dots are the numerical evaluation of the exact norm (15) for the equilateral tetrahedron ( $j_i = j$  for all  $i$ ), for different values of the spin  $j$ . The line is the analytic calculation of the leading order (26). *Right panel:* an open case with  $j_i = j$  for all  $i$  but the normals not closing. The line is the analytic result (30).

The results reported above show how accurate the saddle point approximation is.

## References

- [1] C. Rovelli. *Quantum Gravity*. (Cambridge University Press, Cambridge 2004.)
- [2] J.W. Barrett, L. Crane: “Relativistic spin networks and quantum gravity”, J. Math. Phys. **39** (1998) 3296 [arXiv:gr-qc/9709028].
- [3] E. Bianchi, L. Modesto, C. Rovelli and S. Speziale, “Graviton propagator in loop quantum gravity,” Class. Quant. Grav. **23** (2006) 6989 [arXiv:gr-qc/0604044].  
E. Alesci and C. Rovelli, “Graviton propagator: the nondiagonal terms,” to appear.
- [4] C. Rovelli: “The Basis of the Ponzano-Regge-Turaev-Viro-Ooguri quantum gravity model in the loop representation basis”, Phys. Rev. **D48** (1993) 2702.
- [5] H. Sahlmann, T. Thiemann and O. Winkler, “Coherent states for canonical quantum general relativity and the infinite tensor product extension,” Nucl. Phys. B **606**, 401 (2001) [arXiv:gr-qc/0102038].  
A. Ashtekar, L. Bombelli and A. Corichi, “Semiclassical states for constrained systems,” Phys. Rev. D **72**, 025008 (2005) [arXiv:gr-qc/0504052].

- K. Giesel and T. Thiemann, “Algebraic quantum gravity (AQG). II: Semiclassical analysis,” arXiv:gr-qc/0607100.
- [6] C. Rovelli and S. Speziale, “A semiclassical tetrahedron,” *Class. Quant. Grav.* **23** (2006) 5861 [arXiv:gr-qc/0606074].
  - [7] J. Engle, R. Pereira and C. Rovelli, “The loop-quantum-gravity vertex-amplitude,” arXiv:0705.2388 [gr-qc].
  - [8] J. W. Barrett, “The Classical Evaluation Of Relativistic Spin Networks,” *Adv. Theor. Math. Phys.* **2** (1998) 593 [arXiv:math.qa/9803063].
  - [9] A. Barbieri, “Quantum tetrahedra and simplicial spin networks,” *Nucl. Phys. B* **518** (1998) 714 [arXiv:gr-qc/9707010].
  - [10] L. Freidel and D. Louapre, “Asymptotics of 6j and 10j symbols,” *Class. Quant. Grav.* **20** (2003) 1267 [arXiv:hep-th/0209134].
  - [11] C. Rovelli, “Graviton propagator from background-independent quantum gravity,” *Phys. Rev. Lett.* **97** (2006) 151301 [arXiv:gr-qc/0508124].
  - [12] E. R. Livine and S. Speziale, “Group integral techniques for the spinfoam graviton propagator,” *JHEP* **0611** (2006) 092 [arXiv:gr-qc/0608131].
  - [13] E. R. Livine and S. Speziale, unpublished. See also S. Speziale, “Towards the graviton and the photon from spinfoams,” PhD thesis, 2005.
  - [14] J.F. Plebanski: “On the separation between Einsteinien substructure”, *J. Math. Phys.* **12** (1977) 2511.
  - [15] M. P. Reisenberger, “A left-handed simplicial action for euclidean general relativity,” *Class. Quant. Grav.* **14** (1997) 1753 [arXiv:gr-qc/9609002].
  - [16] A. Perez: “Spin foam quantization of SO(4) Plebanski’s action”, *Adv. Theor. Math. Phys.* **5** (2002) 947 [Erratum-ibid. **6** (2003) 593] [arXiv:gr-qc/0203058].
  - [17] E. Buffenoir, M. Henneaux, K. Noui, Ph. Roche, *Hamiltonian Analysis of Plebanski Theory*, *Class.Quant.Grav.* **21** (2004) 5203-5220 [arXiv:gr-qc/0404041]
  - [18] M. P. Reisenberger, “A lattice worldsheet sum for 4-d Euclidean general relativity,” arXiv:gr-qc/9711052.
  - [19] L. Freidel, K. Krasnov, *Spin Foam Models and the Classical Action Principle*, *Adv.Theor.Math.Phys.* **2** (1999) 1183-1247, [arXiv:hep-th/9807092]
  - [20] M.P. Reisenberger, *On relativistic spin network vertices*, *J.Math.Phys.* **40** (1999) 2046-2054 [arXiv:gr-qc/9809067]

- [21] A. Ashtekar, “Lectures on nonperturbative canonical gravity,” *Singapore, Singapore: World Scientific (1991) 334 p. (Advanced series in astrophysics and cosmology, 6)*
- [22] S. Speziale, “Towards the graviton from spinfoams: The 3d toy model,” JHEP **05** (2006) 039 [arXiv:gr-qc/0512102].  
E. R. Livine, S. Speziale and J. L. Willis, “Towards the graviton from spinfoams: Higher order corrections in the 3d toy model,” Phys. Rev. D **75** (2007) 024038 [arXiv:gr-qc/0605123].
- [23] L. Freidel and E. R. Livine, “Effective 3d quantum gravity and non-commutative quantum field theory,” Phys. Rev. Lett. **96** (2006) 221301 [arXiv:hep-th/0512113].
- [24] M. Bojowald, H. Hernandez, M. Kagan, P. Singh and A. Skrzewski, “Formation and evolution of structure in loop cosmology,” Phys. Rev. Lett. **98** (2007) 031301 [arXiv:astro-ph/0611685].  
A. Ashtekar, T. Pawłowski, P. Singh and K. Vandersloot, “Loop quantum cosmology of  $k = 1$  FRW models,” Phys. Rev. D **75** (2007) 024035 [arXiv:gr-qc/0612104].
- [25] A. Ashtekar and M. Bojowald, “Quantum geometry and the Schwarzschild singularity,” Class. Quant. Grav. **23** (2006) 391 [arXiv:gr-qc/0509075].
- [26] L. Modesto, “Loop quantum black hole,” Class. Quant. Grav. **23** (2006) 5587 [arXiv:gr-qc/0509078].  
L. Modesto, “Gravitational collapse in loop quantum gravity,” arXiv:gr-qc/0610074.
- [27] A. M. Perelomov, *Generalized Coherent States and Their Applications* (Springer-Verlag, 1986).
- [28] D. M. Brink and G. R. Satchler, *Angular Momentum* (Oxford University Press, 1994).